

MITracker: Multi-View Integration for Visual Object Tracking

Mengjie Xu^{1*} Yitao Zhu^{1*} Haotian Jiang¹ Jiaming Li¹ Zhenrong Shen²
Sheng Wang^{1,2} Haolin Huang¹ Xinyu Wang¹ Qing Yang^{1,3} Han Zhang^{1,3} Qian Wang^{1,3†}

¹School of Biomedical Engineering & State Key Laboratory of
Advanced Medical Materials and Devices, ShanghaiTech University

²School of Biomedical Engineering, Shanghai Jiao Tong University

³Shanghai Clinical Research and Trial Center

{xumj2023, zhuyt, jianght2023, lijm2024}@shanghaitech.edu.cn

{zhenrongshen, wsheng}@sjtu.edu.cn

{huanghl2023, wangxy42023, yangqing, zhanghan2, qianwang}@shanghaitech.edu.cn

Abstract

*Multi-view object tracking (MVOT) offers promising solutions to challenges such as occlusion and target loss, which are common in traditional single-view tracking. However, progress has been limited by the lack of comprehensive multi-view datasets and effective cross-view integration methods. To overcome these limitations, we compiled a **Multi-View object Tracking (MVTrack)** dataset of 234K high-quality annotated frames featuring 27 distinct objects across various scenes. In conjunction with this dataset, we introduce a novel MVOT method, **Multi-View Integration Tracker (MITracker)**, to efficiently integrate multi-view object features and provide stable tracking outcomes. MITracker can track any object in video frames of arbitrary length from arbitrary viewpoints. The key advancements of our method over traditional single-view approaches come from two aspects: (1) MITracker transforms 2D image features into a 3D feature volume and compresses it into a bird's eye view (BEV) plane, facilitating inter-view information fusion; (2) we propose an attention mechanism that leverages geometric information from fused 3D feature volume to refine the tracking results at each view. MITracker outperforms existing methods on the MVTrack and GMTD datasets, achieving state-of-the-art performance. The code and the new dataset will be available at mii-laboratory.github.io/MITracker.*

1. Introduction

Visual object tracking, a core computer vision task, involves estimating class-agnostic target positions across video se-

* These authors contributed equally. † Corresponding author.

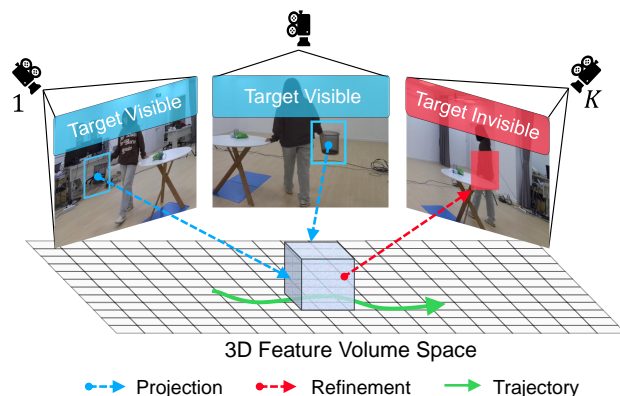


Figure 1. Overview of MITracker’s multi-view integration mechanism. Given K camera views, our method projects features from views with visible targets into a 3D feature volume space, which is then used to refine tracking in views where the target is occluded.

quences. This technique is crucial for applications such as augmented reality and autonomous driving, where it is essential to continuously monitor and predict the trajectories of various objects within dynamic environments. Despite notable advances in single-view tracking through Siamese networks [10, 25] and transformers [3, 9, 46], significant challenges persist – particularly occlusions, appearance changes, and target loss. While approaches like RTracker [22] attempt to address these challenges by determining target loss and detection mechanisms, the inherent limitations of single viewpoint information remain a fundamental constraint.

Multi-camera systems offer a promising solution by leveraging complementary viewpoints to maintain continuous tracking, particularly for handling occlusions through camera overlap [48]. However, the development of effective

multi-view object tracking (MVOT) faces several critical challenges. First, existing multi-view datasets are largely restricted to specific object categories like humans or birds [15, 40], limiting their applicability for generic object tracking. Second, current MVOT approaches [17, 19, 42] primarily focus on tracking specific categories of objects using detection and re-identification methods, which are not suitable for class-agnostic object tracking. Even when attempting to track generic objects across multiple views, researchers have to rely on single-view datasets for training due to the absence of comprehensive multi-view data [38]. This limitation severely restricts models’ ability to understand complex spatial relationships and appearance variations across different viewpoints.

To address these challenges, we first construct a **Multi-View object Tracking** (MVTrack) dataset. MVTrack dataset contains 234K frames captured from 3-4 cameras, with precise bounding box (BBox) annotations covering 27 distinct objects across 9 challenging tracking attributes such as occlusion and deformation. Unlike existing datasets such as GMTD [38] which only provides testing data, MVTrack dataset offers both training and evaluation sets, enabling development and validation of MVOT models.

To effectively utilize MVTrack dataset, we propose a novel MVOT method named **Multi-View Integration Tracker** (MITracker) for tracking any object in video frames of arbitrary length from arbitrary viewpoints. As illustrated in Figure 1, MITracker can integrate multi-view features into a unified 3D feature volume and further refine tracking in occluded views, thus producing robust tracking outcomes. The framework of MITracker consists of two important modules: **View-Specific Feature Extraction** and **Multi-View Integration**. The first module employs a Vision Transformer (ViT) [12] to extract view-specific features of the target object from the current search frame in a streaming manner, where the target object is indicated by a reference frame. The second module constructs a 3D feature volume by fusing 2D features from multiple views and leveraging bird’s eye View (BEV) guidance, which significantly enhances the model’s spatial understanding. This 3D feature volume is then deployed in spatial-enhanced attention to improve tracking accuracy. MITracker allows for the maintenance of stable tracking results and demonstrates strong recovery capabilities in challenging cases such as occlusions and out of view objects.

In summary, our main contributions are as follows:

- We introduce MVTrack, a large-scale multi-view tracking dataset containing 234K frames from 3-4 calibrated cameras. It has precise BBox annotations of 27 object categories across 9 challenging tracking attributes, which provides the first comprehensive benchmark for training class-agnostic MVOT methods and enriches the approaches for evaluating these methods.

- We propose MITracker, a novel multi-view tracking method that constructs BEV-guided 3D feature volumes to enhance spatial understanding and utilize a spatial-enhanced attention mechanism to enable robust recovery from target loss in specific views.
- Our extensive experiments demonstrate that MITracker achieves state-of-the-art (SOTA) performance on both MVTrack and GMTD datasets, improving recovery rate from 56.7% to 79.2% to reduce target loss in challenging scenarios.

2. Related Work

2.1. Visual Object Tracking

Visual object tracking has garnered significant research interest, leading to many breakthroughs. Numerous single-view datasets [13, 20, 21, 23, 24, 27, 29, 36, 39] span a wide range of categories, aimed at enhancing models’ ability to track arbitrary objects. With the expansion of these datasets, single-view tracking methods have also advanced rapidly. Early approaches based on Siamese networks [10, 25] use CNNs to extract features from reference and search regions, establishing a linear relationship between them. More recent works have incorporated transformers for enhanced feature extraction [9, 43], while others introduce attention modules to enable nonlinear relationships [5]. However, these methods lack temporal continuity as they process each frame independently. Algorithms like dynamic template updating [6] and spatio-temporal trajectory tracking [37, 46] have shown promising results in addressing this issue. Despite these advancements, recovering from target loss remains a significant challenge.

To re-track the target after a tracking failure, RTracker [22] leverages a tree-structured memory system to detect target loss and a dedicated detector for self-recovery. However, this approach is constrained by its complex design and the detector’s reliance on specific categories. Single-view tracking suffers from inherent limitations due to its restricted field of view, which is an inevitable challenge. In contrast, GMT [38] incorporates multi-view tracking within a single-view training framework. This limits its capacity to effectively model the intricate relationships between multi-view appearances and background contexts in the real world.

2.2. Multi-View Object Tracking

MVOT provides more comprehensive information about the target, effectively addressing issues such as occlusion. To leverage multi-view information, various fusion strategies have been developed for target association across viewpoints. Some approaches establish multi-view relationships by projecting detection results onto a BEV plane [42]. However, this method is prone to detection errors, especially

Benchmark	Aim	Camera	Class	Total Frames	Videos	Mean Frames	Absent label	Att.	Overlap	Move	Calib.
OTB 2015 [39]	Eva.	1	16	59K	100	590	✗	11	-	-	-
NfS [23]	Eva.	1	17	383K	100	3,830	✗	9	-	-	-
VOT 2017 [24]	Eva.	1	24	21K	60	356	✗	24	-	-	-
TrackingNet [27]	Tra./Eva.	1	27	14.43M	30,643	471	✗	15	-	-	-
LaSOT [13]	Tra./Eva.	1	70	3.52M	1,400	2,053	✓	14	-	-	-
GOT-10k [21]	Tra./Eva.	1	563	1.45M	9,935	149	✓	6	-	-	-
TNL2K [36]	Tra./Eva.	1	-	1.24M	2,000	622	✓	17	-	-	-
VideoCube [20]	Tra./Eva.	1	89	7.46M	500	4,008	✓	12	-	-	-
VastTrack [29]	Tra./Eva.	1	2,115	4.20M	50,610	83	✓	10	-	-	-
CAMPUS [†] [42]	Eva.	4	1	83K	16	5,188	-	-	✓	✗	✗
Wildtrack [†] [4]	Eva.	7	1	2.80K	7	401	-	-	✓	✗	✓
MMPTRACK [†] [15]	Tra./Eva.	4-6	1	2.98M	-	-	-	-	✓	✗	✓
DIVOTrack [†] [16]	Tra./Eva.	3	1	81K	75	1,080	-	-	✓	✓	✗
GMTD [38]	Eva.	2-3	8	18K	23	764	✗	6	✓	✓	✗
MVTrack (Ours)	Tra./Eva.	3-4	27	234K	260	901	✓	9	✓	✗	✓

Table 1. Comparison of current datasets for object tracking. The upper part of the table focuses on single-view datasets, while the lower part is dedicated to multi-view datasets. Datasets marked with [†] are designed for multi-object tracking, the others are for visual object tracking. ‘Tra.’ and ‘Eva.’ indicate training and evaluation, respectively. ‘-’ denotes not available, ‘Att.’ stands for attributes, ‘Overlap’ refers to the overlapping of multi-view images, ‘Move’ indicates the movement of the camera position, and ‘Calib.’ represents calibration.

with occlusion. To tackle this issue, methods [18, 19] improve it by incorporating multi-view information at the detection stage (known as early fusion) through feature projection onto the ground plane, enabling the model to capture richer interaction information across views. Building on these approaches, methods such as [17, 33, 34] map features into 3D space at multiple heights, which reduces distortions caused by ground plane projection.

While these methods enhance multi-view tracking, existing multi-view datasets are relatively scarce and often limited to specific target categories, such as pedestrians [4, 15, 16]. This results in a reliance on detection outcomes, limiting the ability to track arbitrary objects. GMTD [38] expands the target to multiple categories, but its scale remains small, primarily designed for evaluation purposes. There is a pressing need for a multi-view tracking dataset capable of handling arbitrary objects.

3. MVTrack Dataset

MVTrack dataset is designed to fill the gaps in the field of MVOT and has received approval for data collection from an Institutional Review Board. As shown in Table 1, compared to single-view datasets, we maintain competitive class diversity while adding multi-view capabilities. Compared to MVOT datasets, we provide significantly richer object categories (27 vs 1-8 classes) and more videos (260) with practical camera setups (3-4 views). MVTrack dataset is the only dataset that combines multi-view tracking, rich object categories, absent label annotations, and calibration information.

Data Collection. We employ a multi-camera system

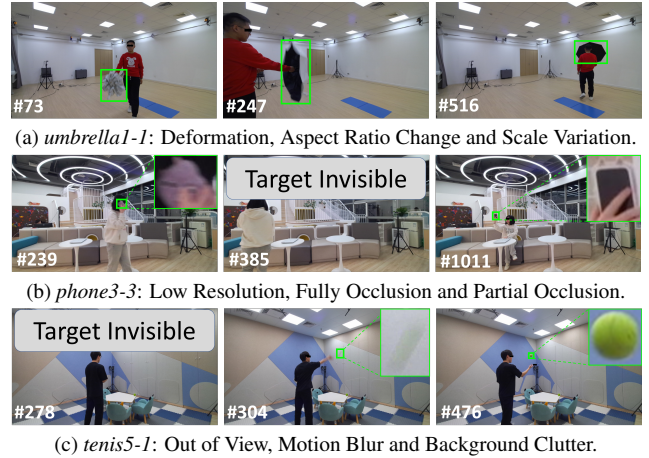


Figure 2. Example sequences, annotations, and their corresponding tracking attributes in the MVTrack dataset.

for data collection, consisting of 3 or 4 time-synchronized Azure Kinect cameras. All video sequences are recorded at a resolution of 1920×1080 with 30 FPS. These cameras are positioned to ensure multiple overlapping views, and their intrinsic parameters are provided by the manufacturer. The extrinsic parameters are obtained through calibration and finely adjusted using MeshLab [7, 8]. With this calibration information, we set the central point of the scene as the origin of the world coordinate system, aligning all viewpoints to this unified coordinate system.

Data Annotation. MVTrack dataset provides frame-level annotations, including 2D object BBoxes and ground coordinate annotations in a unified coordinate system (i.e.,

BEV annotations). Following an annotation strategy similar to LaSOT [13], where for each visible frame, an axis-aligned BBox tightly encloses the target, and an ‘invisible’ label is assigned for the invisible target. The BBox annotations are generated semi-automatically, with trackers [6, 41, 46] used for initial labeling. The machine-generated annotations are then manually adjusted and double-checked for accuracy. Subsequently, using camera calibration parameters, the 2D object BBoxes from multiple viewpoints are projected into the unified coordinate system to compute the BEV coordinates.

Challenging Attributes. In our dataset, we particularly focus on 9 common tracking challenges to better assess tracker performance: Background Clutter, Motion Blur, Partial Occlusion, Full Occlusion, Out of View, Deformation, Low Resolution, Aspect Ratio Change, and Scale Variation.

More specifically, Figure 2 illustrates three challenging samples in the MVTrack dataset. Figure 2a shows significant deformation and scale changes of an umbrella being opened. Figure 2b demonstrates the tracking of small, low-resolution objects like a mobile phone under full and partial occlusions. Figure 2c highlights the impact of fast motion causing blur when tracking a tennis ball. These attributes can significantly aid in training the model to achieve more robust results.

Statistical Analysis. MVTrack dataset consists of five indoor scenes, captured with a total of ten sets of calibration parameters. It covers 27 everyday objects, ranging from small objects like pens to larger objects such as umbrellas. The dataset includes 68 sets of multi-view data, comprising 260 videos and a total of 234,430 frames.

We divide the dataset into training, validation, and testing sets. The training set consists of 196 videos and 180K frames, while the validation set contains 30 videos and 28K frames. The testing set comprises 34 videos and 26K frames. We include an unseen scene in the validation and testing sets that are distinct from the scenes in the training set. Furthermore, the testing set includes both object categories that appear in the training set and new object categories not present during training. This enables evaluation of the model’s performance across various targets and settings.

More details about MVTrack dataset are provided in the Appendix.

4. MITracker

We propose MITracker, a novel multi-view tracking framework that robustly tracks class-agnostic objects across multiple camera views. As illustrated in Figure 3, MITracker consists of two main components: (1) a **view-specific feature extraction** module (Sec. 4.1) that encodes frame features and generates single-view tracking results in a stream-

ing fashion, and (2) a **multi-view integration** module (Sec. 4.2) that fuses multi-view features with BEV guidance and refines view-specific feature with a spatial-enhanced attention mechanism.

4.1. View-Specific Feature Extraction

As shown in Figure 3a, this module processes the video stream from a specific viewpoint k , and extracts target-aware features in the search frame at a timepoint t based on the reference frame that indicates the target object.

View-Specific Encoder. We employ ViT as the backbone of our view-specific encoder. The visual inputs of the view-specific encoder consist of a search frame $S \in \mathbb{R}^{3 \times H_s \times W_s}$ and a reference frame $R \in \mathbb{R}^{3 \times H_r \times W_r}$. As the transformer block processes a series of tokens, we segment the frames into non-overlapping patches with $p \times p$ resolution. The search and reference frames are individually embedded into a token sequence, represented by $I_S \in \mathbb{R}^{N_s \times D}$ and $I_R \in \mathbb{R}^{N_r \times D}$, where D is the hidden dimension, $N_s = \frac{H_s W_s}{p^2}$ is the number of search tokens, and $N_r = \frac{H_r W_r}{p^2}$ is the number of reference tokens.

To ensure temporal continuity between frames, akin to the method utilized in ODTrack [46], two specialized temporal tokens are also included in the inputs of the view-specific encoder to facilitate the propagation of temporal information. Specifically, at any given time t , a learnable token T_t is randomly initialized, which is designed to capture temporal information of the current frame. Concurrently, we incorporate a token T_{t-1} that carries temporal information from the preceding frame, which leverages historical features to enhance tracking accuracy and continuity. The input token sequence of our view-specific encoder can be formulated as the composition of the visual and temporal tokens $f = [T_t, T_{t-1}, I_R, I_S]$, while the output token sequence is denoted as $f' = [T'_t, T'_{t-1}, I'_R, I'_S]$.

After obtaining f' , T'_t is used to compute attention weights in conjunction with I'_S to utilize temporal information for adjustments, which can be described as follows:

$$I_U = I'_S \cdot (I'_S \times (T'_t)^\top), \quad (1)$$

where I_U represents the extracted feature that encapsulates attention focused on the target object in the search frame.

Single-View Tracking Result. We employ a BBox head based on the CenterNet architecture [47] to output tracking results from the extracted feature I_U . This head comprises three distinct sub-networks, each designed to compute the classification score map, BBox dimensions, and offset sizes, respectively. The highest-scoring position on the classification score map is identified as the target location. This configuration establishes a robust framework capable of effectively handling single-view visual object tracking tasks.

To facilitate further multi-view integration, we also apply convolutional layers to map I_U to a 2D feature map

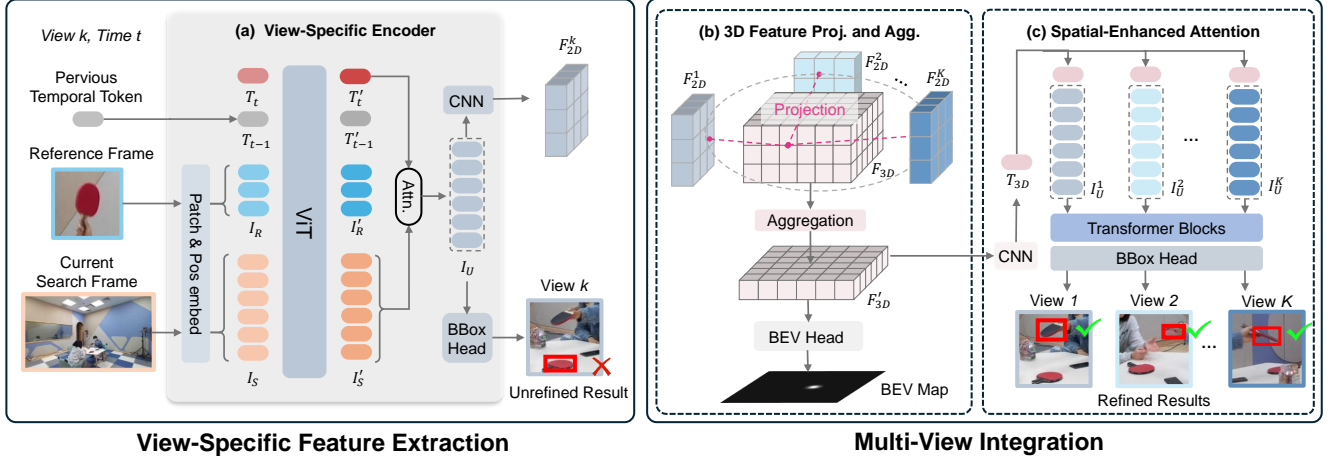


Figure 3. The framework of MITracker. (a) The view-specific feature extraction module employs a ViT that utilizes temporal tokens to process each view independently, outputting unrefined results that can be further improved by multi-view information. The multi-view integration module contains (b) 3D feature volume construction that aggregates features into 3D space with BEV guidance and (c) spatial-enhanced attention that refines tracking results by 3D spatial information.

with original image size, denoted as $F_{2D} \in \mathbb{R}^{32 \times H_s \times W_s}$. This establishes a pixel-wise correspondence between the extracted feature and the search image, which is crucial for reconstructing the 3D feature space in the following section.

4.2. Multi-View Integration

To effectively integrate 2D feature maps $F_{2D}^1, F_{2D}^2, \dots, F_{2D}^K$ from K viewpoints, we project them into a 3D feature space and then aggregate them under the supervision of BEV guidance. Finally, we embed the aggregated feature to a 3D-aware token to refine all view-specific features $I_U^1, I_U^2, \dots, I_U^K$ via spatial-enhanced attention, thus producing stable tracking results across different viewpoints.

3D Feature Projection. As illustrated in Figure 3b, we construct a 3D feature volume of size $X \times Y \times Z$, where (X, Y) represents the horizontal plane and Z axis denotes the vertical direction following [17, 44]. For a viewpoint k , we project the (u, v) coordinates in F_{2D}^k to (x, y, z) coordinates in the 3D feature volume by the formula below:

$$\begin{pmatrix} u \\ v \\ 1 \end{pmatrix} = C_K [C_R | C_t] \begin{pmatrix} x \\ y \\ z \\ 1 \end{pmatrix}, \quad (2)$$

where C_K represents the camera’s intrinsic matrix, C_R denotes the rotation matrix describing the camera’s orientation, and C_t is the translation vector specifying the camera’s position in space. Upon establishing the mapping matrix, we implement bilinear sampling to populate the 3D feature volume. In scenarios that involve multiple viewpoints, we compute the average of the mapped values from each view to ensure consistency. Consequently, we derive a 3D feature volume represented as $F_{3D} \in \mathbb{R}^{32 \times X \times Y \times Z}$.

3D Feature Aggregation. To better integrate multi-view spatial information, we apply 1D convolutional layers to aggregate features along the Z -axis of F_{3D} , resulting in $F'_{3D} \in \mathbb{R}^{32 \times X \times Y}$, thereby consolidating spatial information within the (X, Y) plane. Subsequently, a classification head (i.e., BEV head) is employed to generate a BEV score map from F'_{3D} . This BEV map delineates the object positions on the horizontal plane, thereby imposing supervision constraints on information fusion across multiple viewpoints. This integrative approach allows for precise localization and mapping within multi-view scenarios.

Spatial-Enhanced Attention. BEV guidance for the aggregated 3D feature F'_{3D} only implicitly constrains the original single-view output, but it is insufficient to address the potential target loss issue due to the lack of direct supervision on tracking results. To remedy this, we introduce spatial-enhanced attention to explicitly incorporate F'_{3D} into the tracking process as shown in Figure 3c.

We first use convolutional layers to embed F'_{3D} into a 3D-aware token $T_{3D} \in \mathbb{R}^{1 \times D}$, which inherits multi-view spatial information. For all the K viewpoints, we then individually concatenate T_{3D} with their unrefined features $I_U^1, I_U^2, \dots, I_U^K$ produced by the view-specific encoder. For a viewpoint k , a series of transformer blocks take in its composite token sequence (T_{3D}, I_U^k) and refine them using attention mechanisms that leverage fused 3D spatial information. A final BBox head outputs the refined tracking results, where potential errors such as target loss are corrected.

Dataset	MVTrack						GMTD		
Method	Single-View			Multi-View			Single-View		
	AUC(%)	P _{Norm} (%)	P(%)	AUC(%)	P _{Norm} (%)	P(%)	AUC(%)	P _{Norm} (%)	P(%)
DiMP [1]	43.14	59.52	53.13	35.77	49.04	51.65	52.71	68.24	66.04
PrDiMP [10]	48.61	66.09	58.93	38.49	54.68	57.95	57.76	76.21	70.49
TrDiMP [35]	50.54	67.67	60.44	39.71	55.31	58.52	59.51	78.94	73.48
MixFormer [9]	57.59	75.44	67.72	43.29	58.07	62.70	62.03	82.60	78.48
OSTrack [43]	60.04	77.72	70.06	<u>49.10</u>	<u>65.19</u>	67.34	58.44	77.37	73.23
GRM [14]	52.53	69.91	62.31	41.47	57.33	58.76	55.67	74.02	70.27
SeqTrack [6]	58.37	76.63	69.03	43.88	59.11	63.60	62.97	83.20	79.32
ARTrack [37]	53.23	70.25	62.49	42.52	58.00	60.50	59.56	78.12	74.23
HIPTTrack [2]	60.45	78.92	70.53	48.43	63.69	66.26	62.20	80.62	76.94
EVPTTrack [32]	61.37	79.76	71.97	46.36	61.84	67.20	<u>63.89</u>	<u>83.76</u>	<u>79.93</u>
AQATrack [41]	61.93	80.00	72.69	45.24	59.76	65.33	63.57	83.04	79.44
ODTrack [46]	<u>63.36</u>	<u>82.25</u>	<u>74.46</u>	48.05	63.55	<u>67.70</u>	61.43	82.37	78.35
SAM2* [30]	46.49	63.12	56.82	39.08	53.49	57.34	59.88	74.66	73.25
SAM2Long* [11]	55.30	72.84	67.40	45.40	59.12	65.30	62.80	78.60	77.40
MITracker	68.57	88.77	80.93	71.13	91.87	83.95	65.96	87.05	82.07

Table 2. Comparison with SOTA methods on the MVTrack and GMTD datasets. MITracker is for multi-view tracking, while others are single-view methods. Methods with * use pre-trained weights without fine-tuning. Best results are **bolded**, second-best are underlined.

5. Experiments

5.1. Dataset

In addition to MVTrack dataset, we use two external datasets for training and evaluation, which are detailed as follows.

- **GOT10K.** GOT-10K [21] is a large and diverse dataset with a wide range of object categories. Its training set contains 9,335 videos across 480 moving object categories.
- **GMTD.** GMTD [38] is a multi-view tracking test set with 10 scenes, captured by 2-3 uncalibrated cameras in indoor and outdoor settings. It includes 6 target types and various tracking challenges.

5.2. Implementation Details

Loss Function. For the BBox head, we employ a weighted focal loss [26] L_{cls} for classification, along with the generalized intersection over union loss [31] L_{giou} and L_1 loss for BBox regression. Additionally, a focal loss L_{bev} is utilized for BEV map supervision. The overall loss function of the model is formulated as follows:

$$L_{track} = L_{cls} + \lambda_{giou} L_{giou} + \lambda_{L_1} L_1 + \lambda_{bev} L_{bev}, \quad (3)$$

where $\lambda_{giou} = 5$, $\lambda_{L_1} = 2$, and $\lambda_{bev} = 0.1$ are the coefficients that balance the contributions from each loss.

Training Setup. We initialize our view-specific encoder with pre-trained DINOv2 [28] parameters using the ViT-base model [12]. For the visual inputs, we set the reference frame with 182×182 pixels, and the search frame

with 364×364 pixels. We utilize the camera parameters from the dataset for projection, with the 3D feature volume having dimensions $X = 200$, $Y = 200$, and $Z = 3$.

Our training process consists of two stages. In the first stage, we only train the view-specific feature extraction module. Specifically, we train the view-specific encoder and BBox head using single-view inputs from GOT-10K and MVTrack datasets until convergence. For each viewpoint, we include one reference frame and two random search frames from 200 frame interval in each iteration, thus promoting temporal information propagation between frames. In the second stage, we fine-tune the view-specific encoder and train the entire framework using multi-view data from the MVTrack dataset. For each training sample, we randomly select 2 to 4 viewpoints with one reference and two search frames in each iteration. All the training procedures are conducted on 2 NVIDIA A100 80GB GPUs.

For detailed implementation and training specifics, please refer to the Appendix.

5.3. Evaluation Metrics

We evaluate our method using three standard performance measures from the single-view tracking benchmark [13, 27, 39]: Area Under Curve (AUC), Precision (P), and Normalized Precision (P_{Norm}):

- **AUC:** The Intersection over Union (IoU) measures the overlap between predicted and ground truth BBoxes in each frame. The AUC metric is calculated by varying the IoU threshold to evaluate the area error in the tracking region.

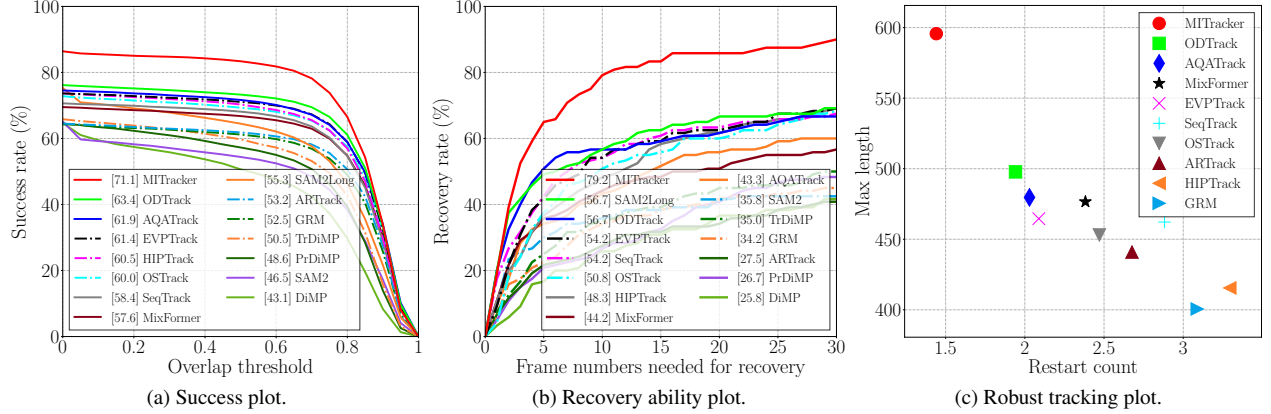


Figure 4. General experiments on the MVTrack dataset evaluate tracking robustness. MITracker provides multi-view results, while other methods yield single-view results. In (a), methods are ranked by AUC and noted in the legend. For (b), the numbers in the legend represent the method’s recovery rate within 10 frames after the target disappears.

- **P**: Precision is defined as the distance between the predicted and ground truth BBox centers. This metric is used to assess the positional error in tracking.
- **P_{Norm}**: To mitigate biases due to variations in BBox size, we normalize the center point by the width and height of the ground truth BBox. This adjustment provides a more accurate metric.

5.4. Comparison with Existing Methods

SOTA Performance on Benchmark. We evaluate tracking performance with single-view visual object tracking methods, training all models (except SAM2 and SAM2Long) on the GOT10K and MVTrack datasets. The models are tested on both the MVTrack and GMTD datasets under single-view and multi-view settings.

However, single-view methods cannot handle multi-view inputs or generate multi-view predictions. To address this, we employ a post-fusion strategy to obtain multi-view results. Specifically, single-view predictions are first projected into the 3D world coordinate system. The region with maximum overlap is identified as the target position, which is then reprojected onto the 2D image plane of each viewpoint to generate the fused multi-view tracking results.

As shown in Table 2, MITracker achieves superior performance in both multi- and single-view tracking across different datasets. In multi-view scenarios with 3-4 cameras, MITracker outperforms other methods that rely on post-processing for multi-view fusion, surpassing the second-best method OStrack by approximately 26% in P_{Norm} . In single-view settings, MITracker surpasses SOTA methods on the MVTrack dataset, achieving an AUC of 68.57%, which outperforms ODTrack by approximately 5%.

Notably, MITracker exhibits strong generalization capabilities by achieving exceptional performance on the GMTD, despite it not being included in the training data.

This demonstrates the robustness of our multi-view approach even in single-view scenarios. We attribute these improvements to our multi-view training strategy, which enables the model to better understand spatial relationships crucial for precise tracking. It is also noteworthy that post-processing degrades the performance of all single-view methods. This indicates a substantial distribution gap in view-independent feature detection across models, making effective fusion through geometric projections challenging.

Stable Continuous Tracking Capability. To further evaluate tracking robustness, we conducted three comparative experiments on the MVTrack dataset. Only MITracker utilizes multi-view inputs, other methods use single-view inputs and generate BBoxes independently.

First, we analyzed tracking success rates across various IoU thresholds, as shown in Figure 4a. MITracker consistently outperforms competing methods regardless of the threshold value.

Second, we evaluated the recovery capability after the target was invisible by measuring the proportion of successful tracking resumption within given frame intervals [22]. As illustrated in Figure 4b, with a 10-frame interval, MITracker achieves a high success rate of 79.2% in these recovery tests. In comparison, SAM2Long only achieves a 56.7% recovery rate under the same setting, highlighting our method’s exceptional ability to quickly reestablish tracking after the target disappears.

In practical applications, users can manually intervene to restart the model’s tracking by providing an accurate initial position. In this experimental setup, we measured the maximum continuous tracking length of video frames and the average number of restarts (triggered when target loss exceeds 10 frames, using ground truth for repositioning) [45]. As shown in Figure 4c, MITracker achieves nearly 100 frames longer tracking duration than ODTrack while

requiring fewer restart counts.

5.5. Ablation Study

Results in Table 3 demonstrate that BEV Loss, which provides implicit multi-view information feedback, significantly enhances model performance. This improvement is attributed to its ability to augment spatial awareness during single-view feature extraction. The Spatial attention, which utilizes fused information to adjust outputs from single-view perspectives, also contributes to notable performance improvements in the model.

BEV Loss	Spatial Attention	AUC(%)	$P_{Norm}(\%)$	P(%)
		63.99	82.82	75.00
✓		69.64	89.85	82.01
✓	✓	71.13	91.87	83.95

Table 3. Ablation study for multi-view evaluation on MVTrack dataset.

5.6. Visualization Comparison

Our qualitative evaluation focuses on the influence of occlusion and fast motion. In the upper part of Figure 5, we select two viewpoints from the MVTrack dataset and evaluate them on MITracker and ODTrack, which has the second-best performance on this dataset. The gray areas in the graph represent periods when the object is out of view or fully occluded by other objects. We can easily observe that MITracker is able to re-track the object shortly after it reappears, whereas ODTrack tends to continue in a lost state. For instances #405 and #515 in V2, even when the object reappears in the frame, ODTrack still mistakenly locks onto the wrong object. The bottom of Figure 5 presents tests conducted on the GMTD, where we also selected the second-best method, EVPTrack, for comparison with MITracker. When a pedestrian reappears after being obscured by a pillar, EVPTrack mistakenly locks onto the wrong target, whereas MITracker is able to maintain stable and continuous tracking.

We also visualize the predicted BEV trajectories from MITracker in Figure 6. Referencing the ground-truth trajectories, MITracker effectively integrates multi-view features and provides accurate 3D spatial information.

6. Discussion

In previous sections, we provide a detailed introduction to the MVTrack dataset and demonstrate the outstanding performance of MITracker. However, there are some areas that could be improved in future work.

Limitations. Although MVTrack dataset includes a diverse set of scenes, it currently consists of indoor environments only, potentially limiting the generalization of meth-



Figure 5. Qualitative comparison results. Comparison of our tracker with two SOTA methods on MVTrack dataset (top) and GMTD (bottom). Each frame is cropped for better visualization. IoU curves of each method’s prediction and ground truth are shown above, where IoU reflects tracking quality. MITracker demonstrates superior re-tracking performance upon target reappearance.

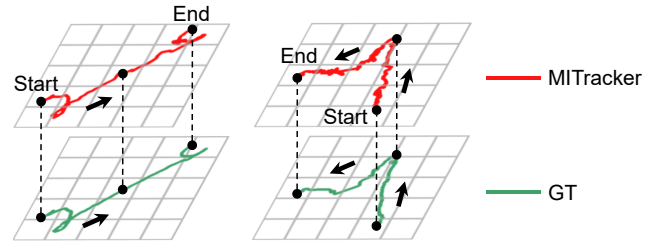


Figure 6. Visualization of BEV trajectories on the MVTrack dataset. Left: scene captured by four cameras. Right: scene captured by three cameras.

ods trained on it to outdoor settings. Additionally, MITracker relies on camera calibration for multi-view fusion, which may restrict its applicability in scenarios where calibration is challenging or infeasible.

Future work. We plan to extend MVTrack dataset by including outdoor scenes and a wider range of tracking objects to enable the development of more generalizable

multi-view tracking algorithms. Furthermore, we aim to enhance MITracker by reducing its dependency on precise camera calibration, making it more adaptable to scenarios where accurate calibration is challenging.

7. Conclusion

In this study, we address key challenges such as occlusion and target loss in MVOT by making two significant contributions: (1) MVTrack, a comprehensive dataset with 234K high-quality annotations across diverse scenes and object categories, and (2) MITracker, a novel visual tracking method that effectively integrates multi-view object features. MITracker achieves SOTA results on MVTrack and GMTD datasets, demonstrating its ability to provide stable and reliable tracking across different viewpoints and video durations. Our contributions lay the foundation for future advancements in MVOT, enabling the development of more robust and accurate tracking systems for real-world scenarios.

8. Acknowledgments

This work was partially supported by STI 2030-Major Projects (2022ZD0209000) and HPC Platform of ShanghaiTech University.

References

- [1] Goutam Bhat, Martin Danelljan, Luc Van Gool, and Radu Timofte. Learning discriminative model prediction for tracking. In *Proceedings of the IEEE/CVF international conference on computer vision*, pages 6182–6191, 2019. 6
- [2] Wenrui Cai, Qingjie Liu, and Yunhong Wang. Hiptrack: Visual tracking with historical prompts. In *Proceedings of the IEEE/CVF Conference on Computer Vision and Pattern Recognition*, 2024. 6
- [3] Yidong Cai, Jie Liu, Jie Tang, and Gangshan Wu. Robust object modeling for visual tracking. In *Proceedings of the IEEE/CVF International Conference on Computer Vision*, pages 9589–9600, 2023. 1
- [4] Tatjana Chavdarova, Pierre Baqué, Stéphane Bouquet, Andrii Maksai, Cijo Jose, Timur Bagautdinov, Louis Lettry, Pascal Fua, Luc Van Gool, and François Fleuret. Wildtrack: A multi-camera hd dataset for dense unscripted pedestrian detection. In *Proceedings of the IEEE conference on computer vision and pattern recognition*, pages 5030–5039, 2018. 3
- [5] Xin Chen, Bin Yan, Jiawen Zhu, Dong Wang, Xiaoyun Yang, and Huchuan Lu. Transformer tracking. In *Proceedings of the IEEE/CVF conference on computer vision and pattern recognition*, pages 8126–8135, 2021. 2
- [6] Xin Chen, Houwen Peng, Dong Wang, Huchuan Lu, and Han Hu. Seqtrack: Sequence to sequence learning for visual object tracking. In *Proceedings of the IEEE/CVF conference on computer vision and pattern recognition*, pages 14572–14581, 2023. 2, 4, 6
- [7] Paolo Cignoni, Alessandro Muntoni, Guido Ranzuglia, and Marco Callieri. MeshLab. 3
- [8] Paolo Cignoni, Marco Callieri, Massimiliano Corsini, Matteo Dellepiane, Fabio Ganovelli, and Guido Ranzuglia. MeshLab: an Open-Source Mesh Processing Tool. In *Eurographics Italian Chapter Conference*. The Eurographics Association, 2008. 3
- [9] Yutao Cui, Cheng Jiang, Limin Wang, and Gangshan Wu. Mixformer: End-to-end tracking with iterative mixed attention. In *Proceedings of the IEEE/CVF conference on computer vision and pattern recognition*, pages 13608–13618, 2022. 1, 2, 6
- [10] Martin Danelljan, Luc Van Gool, and Radu Timofte. Probabilistic regression for visual tracking. In *Proceedings of the IEEE/CVF conference on computer vision and pattern recognition*, pages 7183–7192, 2020. 1, 2, 6
- [11] Shuangrui Ding, Rui Qian, Xiaoyi Dong, Pan Zhang, Yuhang Zang, Yuhang Cao, Yuwei Guo, Dahua Lin, and Jiaqi Wang. Sam2long: Enhancing sam 2 for long video segmentation with a training-free memory tree. *arXiv preprint arXiv:2410.16268*, 2024. 6
- [12] Alexey Dosovitskiy. An image is worth 16x16 words: Transformers for image recognition at scale. *arXiv preprint arXiv:2010.11929*, 2020. 2, 6
- [13] Heng Fan, Liting Lin, Fan Yang, Peng Chu, Ge Deng, Sijia Yu, Hexin Bai, Yong Xu, Chunyuan Liao, and Haibin Ling. Lasot: A high-quality benchmark for large-scale single object tracking. In *Proceedings of the IEEE/CVF conference on computer vision and pattern recognition*, pages 5374–5383, 2019. 2, 3, 4, 6
- [14] Shenyuan Gao, Chunluan Zhou, and Jun Zhang. Generalized relation modeling for transformer tracking. In *Proceedings of the IEEE/CVF Conference on Computer Vision and Pattern Recognition*, pages 18686–18695, 2023. 6
- [15] Xiaotian Han, Quanzeng You, Chunyu Wang, Zhizheng Zhang, Peng Chu, Houdong Hu, Jiang Wang, and Zicheng Liu. Mmptrack: Large-scale densely annotated multi-camera multiple people tracking benchmark. In *Proceedings of the IEEE/CVF Winter Conference on Applications of Computer Vision*, pages 4860–4869, 2023. 2, 3
- [16] Shengyu Hao, Peiyuan Liu, Yibing Zhan, Kaixun Jin, Zuozhu Liu, Mingli Song, Jenq-Neng Hwang, and Gaoang Wang. Divotrack: A novel dataset and baseline method for cross-view multi-object tracking in diverse open scenes. *International Journal of Computer Vision*, 132(4):1075–1090, 2024. 3
- [17] Adam W Harley, Zhaoyuan Fang, Jie Li, Rares Ambrus, and Katerina Fragkiadaki. Simple-bev: What really matters for multi-sensor bev perception? In *2023 IEEE International Conference on Robotics and Automation (ICRA)*, pages 2759–2765. IEEE, 2023. 2, 3, 5
- [18] Yunzhong Hou and Liang Zheng. Multiview detection with shadow transformer (and view-coherent data augmentation). In *Proceedings of the 29th ACM International Conference on Multimedia*, pages 1673–1682, 2021. 3
- [19] Yunzhong Hou, Liang Zheng, and Stephen Gould. Multi-view detection with feature perspective transformation. In

- Computer Vision–ECCV 2020: 16th European Conference, Glasgow, UK, August 23–28, 2020, Proceedings, Part VII 16, pages 1–18. Springer, 2020. 2, 3
- [20] Shiyu Hu, Xin Zhao, Lianghua Huang, and Kaiqi Huang. Global instance tracking: Locating target more like humans. *IEEE Transactions on Pattern Analysis and Machine Intelligence*, 45(1):576–592, 2022. 2, 3
- [21] Lianghua Huang, Xin Zhao, and Kaiqi Huang. Got-10k: A large high-diversity benchmark for generic object tracking in the wild. *IEEE transactions on pattern analysis and machine intelligence*, 43(5):1562–1577, 2019. 2, 3, 6
- [22] Yuqing Huang, Xin Li, Zikun Zhou, Yaowei Wang, Zhenyu He, and Ming-Hsuan Yang. Rtracker: Recoverable tracking via pn tree structured memory. In *Proceedings of the IEEE/CVF Conference on Computer Vision and Pattern Recognition*, pages 19038–19047, 2024. 1, 2, 7
- [23] Hamed Kiani Galoogahi, Ashton Fagg, Chen Huang, Deva Ramanan, and Simon Lucey. Need for speed: A benchmark for higher frame rate object tracking. In *Proceedings of the IEEE international conference on computer vision*, pages 1125–1134, 2017. 2, 3
- [24] Matej Kristan, Jiri Matas, Aleš Leonardis, Tomáš Vojř, Roman Pflugfelder, Gustavo Fernandez, Georg Nebel, Fatih Porikli, and Luka Čehovin. A novel performance evaluation methodology for single-target trackers. *IEEE transactions on pattern analysis and machine intelligence*, 38(11):2137–2155, 2016. 2, 3
- [25] Bo Li, Junjie Yan, Wei Wu, Zheng Zhu, and Xiaolin Hu. High performance visual tracking with siamese region proposal network. In *Proceedings of the IEEE conference on computer vision and pattern recognition*, pages 8971–8980, 2018. 1, 2
- [26] T Lin. Focal loss for dense object detection. *arXiv preprint arXiv:1708.02002*, 2017. 6
- [27] Matthias Muller, Adel Bibi, Silvio Giancola, Salman Alsubaihi, and Bernard Ghanem. Trackingnet: A large-scale dataset and benchmark for object tracking in the wild. In *Proceedings of the European conference on computer vision (ECCV)*, pages 300–317, 2018. 2, 3, 6
- [28] Maxime Oquab, Timothée Darcet, Théo Moutakanni, Huy Vo, Marc Szafraniec, Vasil Khalidov, Pierre Fernandez, Daniel Haziza, Francisco Massa, Alaaeldin El-Nouby, et al. Dinov2: Learning robust visual features without supervision. *arXiv preprint arXiv:2304.07193*, 2023. 6
- [29] Liang Peng, Junyuan Gao, Xinran Liu, Weihong Li, Shaohua Dong, Zhipeng Zhang, Heng Fan, and Libo Zhang. Vast-track: Vast category visual object tracking. *arXiv preprint arXiv:2403.03493*, 2024. 2, 3
- [30] Nikhila Ravi, Valentin Gabeur, Yuan-Ting Hu, Ronghang Hu, Chaitanya Ryali, Tengyu Ma, Haitham Khedr, Roman Rädle, Chloe Rolland, Laura Gustafson, Eric Mintun, Juntao Pan, Kalyan Vasudev Alwala, Nicolas Carion, Chao-Yuan Wu, Ross Girshick, Piotr Dollár, and Christoph Feichtenhofer. Sam 2: Segment anything in images and videos. *arXiv preprint arXiv:2408.00714*, 2024. 6
- [31] Hamid Rezaeifighi, Nathan Tsoi, JunYoung Gwak, Amir Sadeghian, Ian Reid, and Silvio Savarese. Generalized intersection over union: A metric and a loss for bounding box regression. In *Proceedings of the IEEE/CVF conference on computer vision and pattern recognition*, pages 658–666, 2019. 6
- [32] Liangtao Shi, Bineng Zhong, Qihua Liang, Ning Li, Shengping Zhang, and Xianxian Li. Explicit visual prompts for visual object tracking. In *AAAI*, 2024. 6
- [33] Liangchen Song, Jialian Wu, Ming Yang, Qian Zhang, Yuan Li, and Junsong Yuan. Stacked homography transformations for multi-view pedestrian detection. In *Proceedings of the IEEE/CVF International Conference on Computer Vision*, pages 6049–6057, 2021. 3
- [34] Torben Teepe, Philipp Wolters, Johannes Gilg, Fabian Herzog, and Gerhard Rigoll. Earlybird: Early-fusion for multi-view tracking in the bird’s eye view. In *Proceedings of the IEEE/CVF Winter Conference on Applications of Computer Vision*, pages 102–111, 2024. 3
- [35] Ning Wang, Wengang Zhou, Jie Wang, and Houqiang Li. Transformer meets tracker: Exploiting temporal context for robust visual tracking. In *Proceedings of the IEEE/CVF conference on computer vision and pattern recognition*, pages 1571–1580, 2021. 6
- [36] Xiao Wang, Xiujun Shu, Zhipeng Zhang, Bo Jiang, Yaowei Wang, Yonghong Tian, and Feng Wu. Towards more flexible and accurate object tracking with natural language: Algorithms and benchmark. In *Proceedings of the IEEE/CVF conference on computer vision and pattern recognition*, pages 13763–13773, 2021. 2, 3
- [37] Xing Wei, Yifan Bai, Yongchao Zheng, Dahu Shi, and Yihong Gong. Autoregressive visual tracking. In *Proceedings of the IEEE/CVF Conference on Computer Vision and Pattern Recognition*, pages 9697–9706, 2023. 2, 6
- [38] Minye Wu, Haibin Ling, Ning Bi, Shenghua Gao, Qiang Hu, Hao Sheng, and Jingyi Yu. Visual tracking with multi-view trajectory prediction. *IEEE Transactions on Image Processing*, 29:8355–8367, 2020. 2, 3, 6
- [39] Yi Wu, Jongwoo Lim, and Ming-Hsuan Yang. Object tracking benchmark. *IEEE Transactions on Pattern Analysis and Machine Intelligence*, 37:1–1, 2015. 2, 3, 6
- [40] Shiting Xiao, Yufu Wang, Ammon Perkes, Bernd Pfrommer, Marc Schmidt, Kostas Daniilidis, and Marc Badger. Multi-view tracking, re-id, and social network analysis of a flock of visually similar birds in an outdoor aviary. *International Journal of Computer Vision*, 131(6):1532–1549, 2023. 2
- [41] Jinxia Xie, Bineng Zhong, Zhiyi Mo, Shengping Zhang, Liangtao Shi, Shuxiang Song, and Rongrong Ji. Autoregressive queries for adaptive tracking with spatio-temporal transformers. In *Proceedings of the IEEE/CVF Conference on Computer Vision and Pattern Recognition*, pages 19300–19309, 2024. 4, 6
- [42] Yuanlu Xu, Xiaobai Liu, Yang Liu, and Song-Chun Zhu. Multi-view people tracking via hierarchical trajectory composition. In *Proceedings of the IEEE conference on computer vision and pattern recognition*, pages 4256–4265, 2016. 2, 3
- [43] Botao Ye, Hong Chang, Bingpeng Ma, Shiguang Shan, and Xilin Chen. Joint feature learning and relation modeling for tracking: A one-stream framework. In *European Conference on Computer Vision*, pages 341–357. Springer, 2022. 2, 6

- [44] Yifu Zhang, Chunyu Wang, Xinggang Wang, Wenyu Liu, and Wenjun Zeng. Voxeltrack: Multi-person 3d human pose estimation and tracking in the wild. IEEE Transactions on Pattern Analysis and Machine Intelligence, 45(2):2613–2626, 2022. [5](#)
- [45] Xin Zhao, Shiyu Hu, Yipei Wang, Jing Zhang, Yimin Hu, Rongshuai Liu, Haibin Ling, Yin Li, Renshu Li, Kun Liu, et al. Biodrone: A bionic drone-based single object tracking benchmark for robust vision. International Journal of Computer Vision, 132(5):1659–1684, 2024. [7](#)
- [46] Yaozong Zheng, Bineng Zhong, Qihua Liang, Zhiyi Mo, Shengping Zhang, and Xianxian Li. Odtrack: Online dense temporal token learning for visual tracking. In Proceedings of the AAAI Conference on Artificial Intelligence, pages 7588–7596, 2024. [1](#), [2](#), [4](#), [6](#)
- [47] Xingyi Zhou, Dequan Wang, and Philipp Krähenbühl. Objects as points. arXiv preprint arXiv:1904.07850, 2019. [4](#)
- [48] Yitao Zhu, Sheng Wang, Mengjie Xu, Zixu Zhuang, Zhixin Wang, Kaidong Wang, Han Zhang, and Qian Wang. Muc: Mixture of uncalibrated cameras for robust 3d human body reconstruction. arXiv preprint arXiv:2403.05055, 2024. [1](#)

MITracker: Multi-View Integration for Visual Object Tracking

Supplementary Material

Section 9 provides additional information on the MVTrack dataset, while Section 10 includes further implementation details and experimental results of MITracker.

9. Dataset Details

Data Annotation. In the BEV annotations, the MVTrack dataset covers an $8m \times 8m$ area. Ground truth labels are projected onto a 400×400 grid, where each cell is $2cm \times 2cm$ in size.

Attributes Definition. MVTrack dataset contains nine attributes to assess tracking robustness, as shown in Table 4. We provide frame-level binary labels for five attributes: Background Clutter (BC), Motion Blur (MB), Partial Occlusion (POC), Full Occlusion (FOC), and Out of View (OV). These are manually annotated for each frame. Deformation (DEF) is labeled according to whether the tracked target deforms. Low Resolution (LR), Aspect Ratio Change (ARC), and Scale Variation (SV) are automatically computed from changes in the BBox size.

Att.	Definition
BC	The background has similar appearance as the target
MB	The target region is blurred due to target motion
POC	The target is partially occluded in the frame
FOC	The target is fully occluded in the frame
OV	The target completely leaves the video frame
DEF	The target is deformable during tracking
LR	The target BBox is smaller than 1000 pixels
ARC	The ratio of BBox aspect ratio is outside the range [0.5, 2]
SV	The ratio of BBox is outside the range [0.5, 2]

Table 4. Description of 9 attributes in MVTrack dataset.

Statistical Details. The MVTrack dataset contains 260 videos averaging around 900 frames each, as shown in Figure 7a. As illustrated in Figure 7b, a key challenge is occlusion, which often results from subject-object interactions that cause partial or complete occlusion. Consequently, tracking models need to manage occlusion to perform robustly and adeptly on this dataset.

10. Experiment Details

10.1. Training and Resource Analysis

Training Details. We process the visual inputs by cropping the reference frame to 2 times the target’s BBox size and

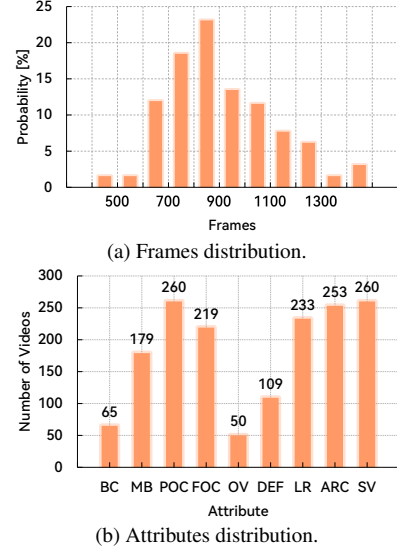


Figure 7. Distribution of sequences in each attribute and length in our MVTrack dataset.

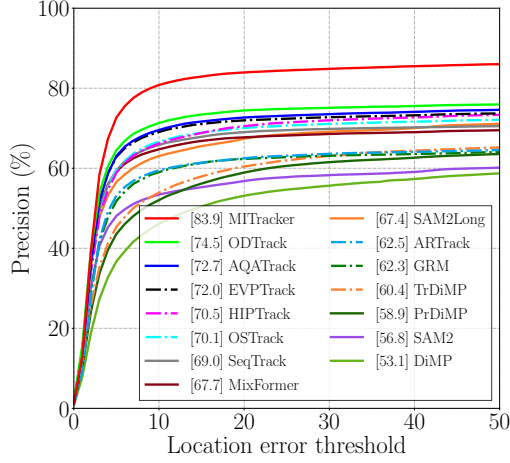
resizing it to 182×182 pixels. The search frame is cropped at 4.5 times the target box area and resized to 364×364 pixels to expand the search region. During projection, we transform the camera intrinsic matrix C_K accordingly and add noise to the translation vector C_t to prevent overfitting in multi-view fusion.

Training consists of two stages. In the first stage, we optimize the view-specific encoder using AdamW with a learning rate of 1×10^{-5} and the rest of the model at 1×10^{-4} . We train for 50 epochs, sampling 10,000 image pairs per epoch with a batch size of 32. In the second stage, we fine-tune the encoder at 1×10^{-6} while keeping other components at 1×10^{-4} . We use the MVTrack dataset, sampling 2,500 multi-view image pairs per epoch for 40 epochs with a batch size of 4. AdamW is used throughout.

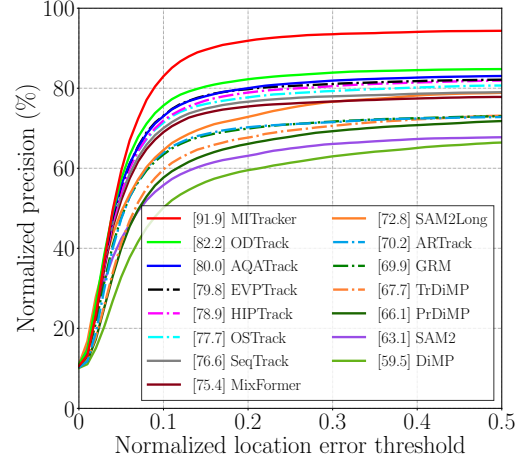
Computational Resource. We evaluate MITracker and the single-view model ODTrack under the same input (4 views) on an NVIDIA A100, as summarized in Table 5. Although multi-view fusion introduces additional computational overhead, it remains within an acceptable range.

Method	Parameters (M)	GRAM (MB)	FPS
ODTrack	92.12	365.82	18.78
MITracker	101.65	407.78	14.08

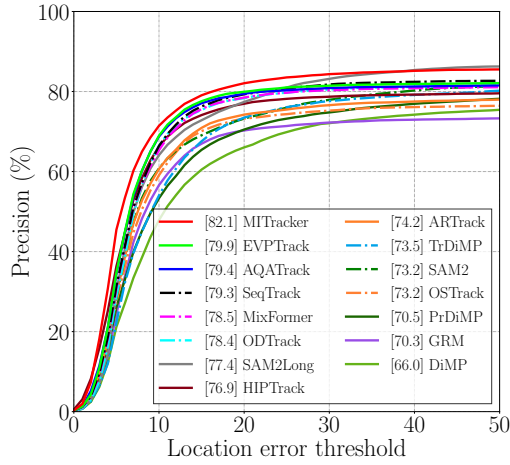
Table 5. Comparison of computational complexity and resource.



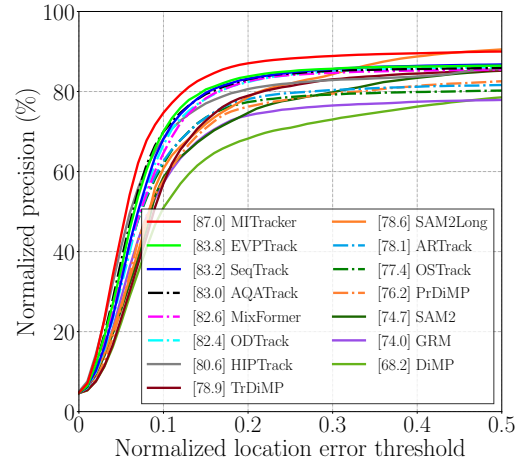
(a) Precision plot on MVTrack dataset.



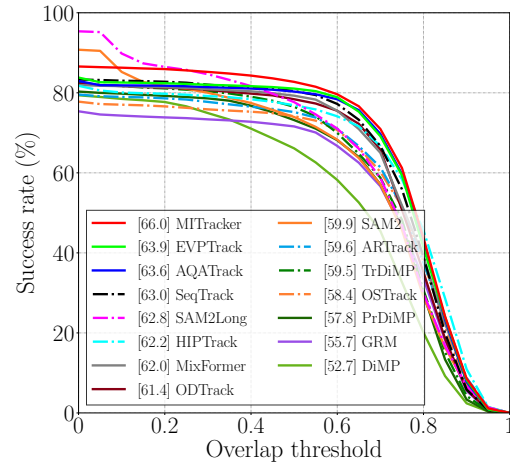
(b) Normalized precision plot on MVTrack dataset.



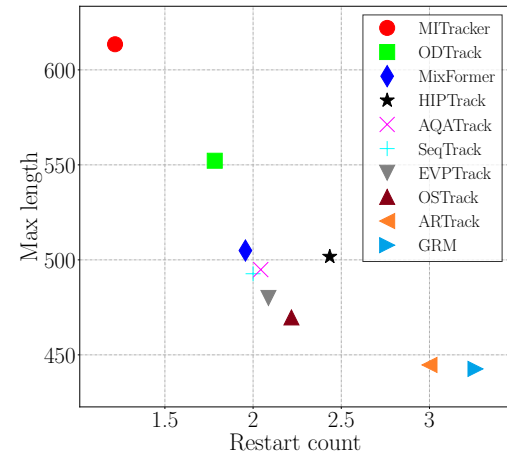
(c) Precision plot on GMTD.



(d) Normalized precision plot on GMTD.



(e) Success plot on GMTD.



(f) Robust tracking plot on GMTD.

Figure 8. Comparative results across MVTrack and GMTD datasets, with rankings noted in the legends. Parts (a) and (c) sort methods by P with a 20-pixel threshold, parts (b) and (d) by P_{norm} with a 0.2 threshold, and part (e) by AUC.

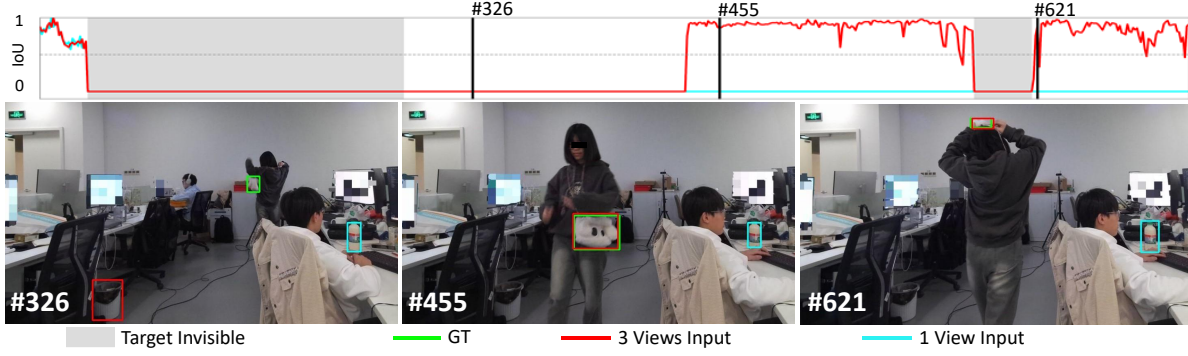


Figure 9. Qualitative comparison results on the impact of different numbers of input views. For a specific view, we compare the effects of using only that view versus including two additional overlapping views.

10.2. Comparison on Benchmark Details

In Figure 8, we provide further quantitative evaluations of the AUC, P, and P_{norm} across various threshold settings for both the MVTrack and GMTD datasets. In most settings, MITracker consistently outperforms other methods.

During zero-shot testing on the GMTD, SAM2 and SAM2Long perform better under lenient threshold conditions but lacks the ability to localize objects precisely. Furthermore, as shown in Figure 8f, MITracker sustains longer tracking durations with fewer reinitializations on this unseen dataset.

10.3. More Ablation Study

Impact of Input Views. To assess the importance of the number of views for tracking, we select a fixed camera from each scenario in the testing set. We then examine how model performance changes as we increase the number of additional cameras. The results in Table 6 highlight the benefits of adding more cameras.

Figure 9 illustrates the challenges faced by the single-view model: after a prolonged target disappearance, it mis-tracks a white bottle. In contrast, the multi-view model initially mistakes a white trash can for the target but quickly recovers and maintains stable tracking with the aid of additional views.

Input views	AUC(%)	$P_{Norm}(\%)$	P(%)
1	62.27	84.71	73.92
2	63.97	87.07	76.30
3	67.97	91.50	80.73
3/4	68.65	92.37	81.55

Table 6. Ablation study for the impact of different numbers of input views on MVTrack dataset.

Impact of Multi-View Training. Our experiment shows that multi-view training improves single-view performance by exposing the model to richer spatial information, which

enhances its ability to handle occlusion and reappearance. Table 7 compares results with MITracker SV trained under single-view settings, highlighting the advantages of multi-view training even for single-view scenarios.

Method	AUC (%)	$P_{Norm}(\%)$	P (%)
MITracker SV	63.42	82.97	79.67
MITracker	65.96	87.05	82.07

Table 7. Zero-shot performance of single-view results on GMTD.

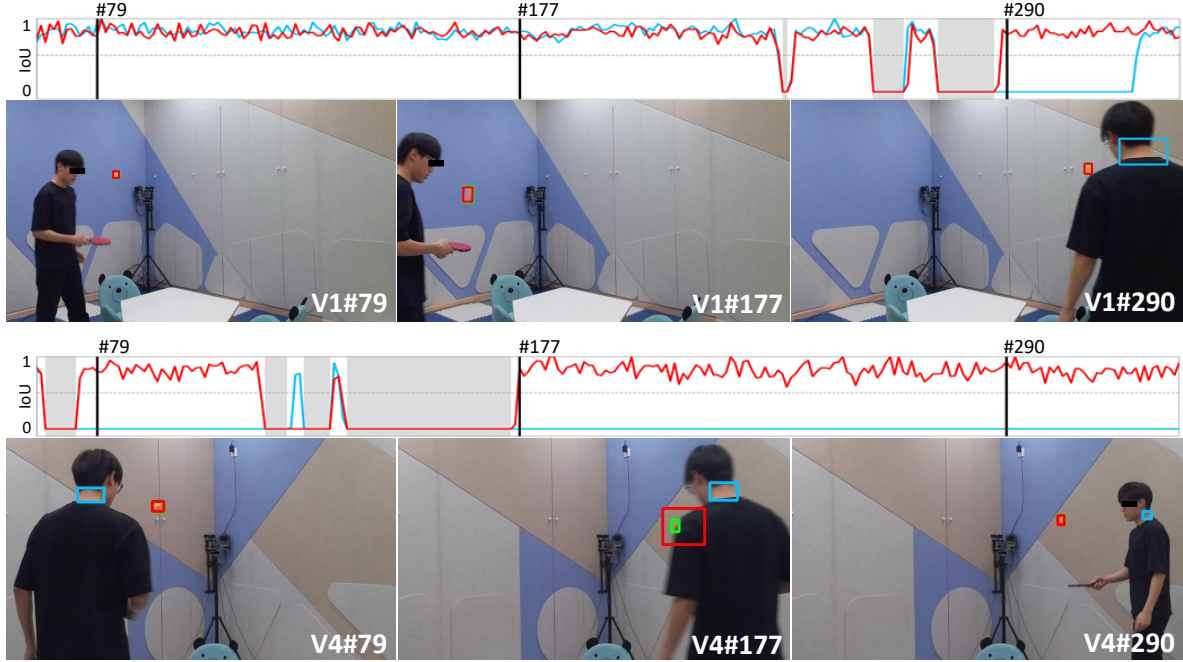
Impact of Temporal Token. The temporal token incorporates tracking information from previous frames, Table 8 highlights the improvements achieved through the temporal token.

Temporal Token	AUC (%)	$P_{Norm}(\%)$	P (%)
	69.30	89.62	81.60
✓	71.13	91.87	83.95

Table 8. Ablation study for temporal token.

10.4. More Visualization Results

We provide additional visual comparison results as illustrated in Figure 10 and Figure 11 from the MVTrack dataset, and Figure 12 from the GMTD. MITracker exhibits enhanced re-tracking capabilities both in multi-view and single-view scenarios. Furthermore, multi-view information assists in correcting instances of mistracking. To facilitate better visualization, each frame is cropped to a fixed area. The IoU curves above further illustrate the tracking accuracy by comparing each method’s predictions to the ground truth.



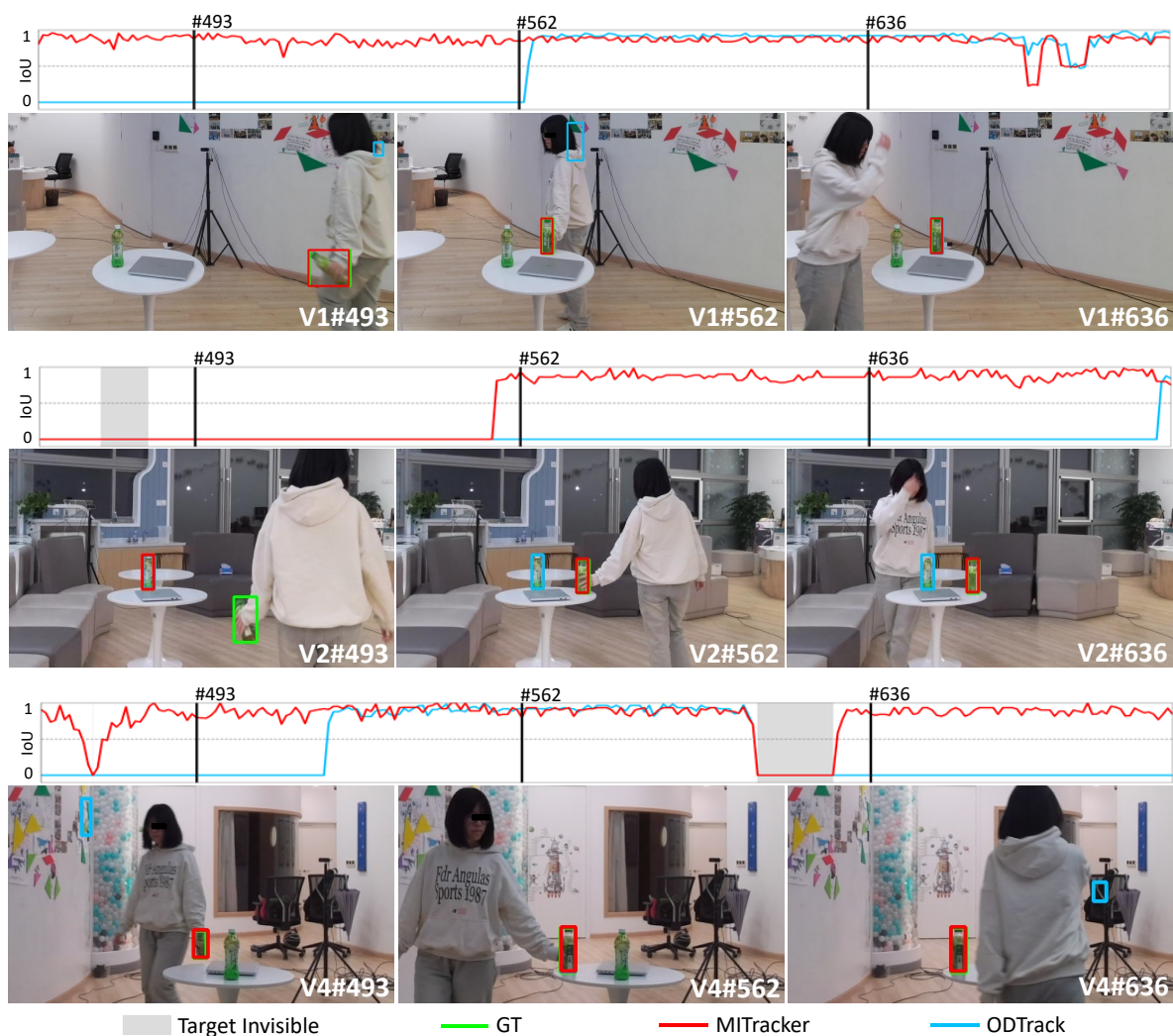
(a) Two views: *pingpong5-1* and *pingpong5-4*. ODTrack tends to lose track after extended periods of target disappearance, whereas MI-Tracker demonstrates robust recovery capabilities.



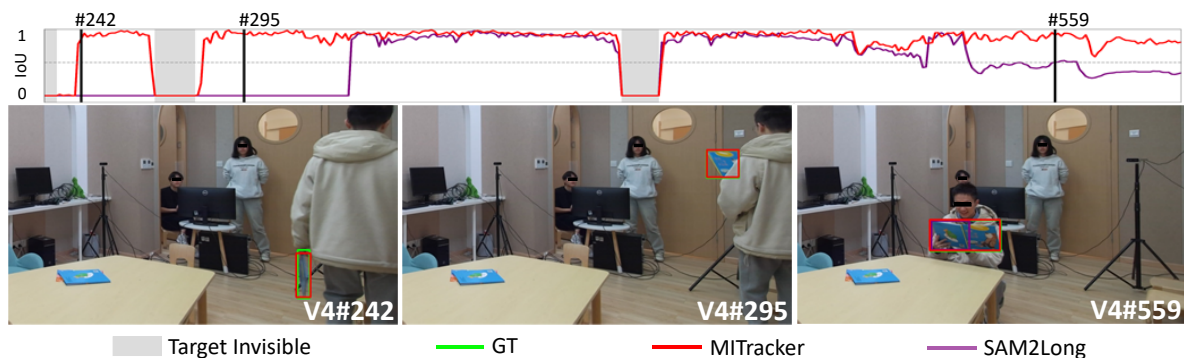
(b) Two views: *umbrella2-1* and *umbrella2-2*. Under the interference of a similar object, ODTrack fails to re-track the correct target. In contrast, with the aid of multi-view assistance, MITracker can correct tracking errors from frame V1#415 to #521.

Target Invisible
 GT
 MITracker
 ODTrack

Figure 10. Qualitative comparison results on the MVTrack dataset using ODTrack.

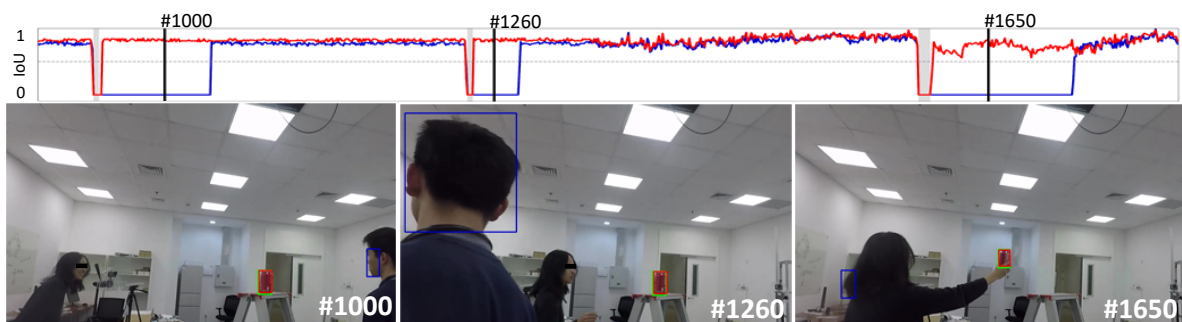


(a) Three views: *bottle3-1*, *bottle3-2* and *bottle3-4*. In V2 #493, MITracker momentarily mistracks a similar object as the target but successfully re-tracks the target by #562. In contrast, ODTrack struggles to recover once it mistracks.

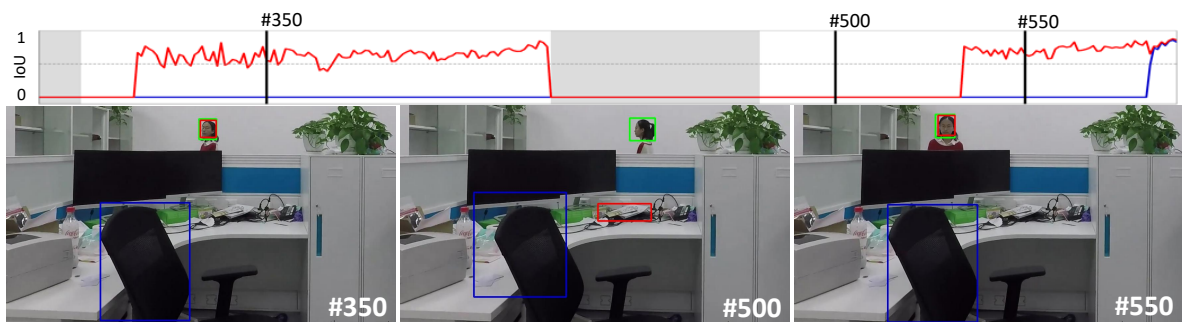


(b) Sequence: *book4-4*. SAM2Long completely loses the target following disappearances at frames #242 and #295. Upon re-tracking, it fails to adapt to target deformation, resulting in diminished IoU by frame #559.

Figure 11. Qualitative comparison results on the MVTrack dataset using ODTrack and SAM2Long.



(a) Sequence: *cola-2*. MITracker demonstrates faster re-tracking capabilities than EVPTrack upon target reappearance.



(b) Sequence: *manInOffice-2*. EVPTrack fails to correct after mistracking. In contrast, MITracker exhibits superior recovery capabilities, as demonstrated between frames #500 and #550.

Target Invisible
 GT
 MITracker
 EVPTrack

Figure 12. Qualitative comparison results on the GMTD using EVPTrack.